SJTU:SPATIAL JUDGMENTS IN MULTIMODAL MODELS - TOWARDS UNIFIED SEGMENTATION THROUGH COORDINATE DETECTION *

JOONGWON CHAE#[1], **Zhenyu Wang#**[1], **Peiwu Qin***[1]

[1]Institute of Biopharmaceutical and Health Engineering, Shenzhen International Graduate School, Tsinghua University, Shenzhen, Guangdong, China
#These authors contributed equally to this work.
*Corresponding authors: pwqin@sz.tsinghua.edu.cn (P. Qin)

ABSTRACT

Despite advances in vision-language understanding, implementing image segmentation within multimodal architectures remains a fundamental challenge in modern artificial intelligence systems. Existing vision-language models, which primarily rely on backbone architectures or CLIP-based embedding learning, demonstrate inherent limitations in fine-grained spatial localization and operational capabilities. This paper introduces SJTU: Spatial Judgments in multimodal models - Towards Unified segmentation through coordinate detection, a novel framework that leverages spatial coordinate understanding to bridge vision-language interaction and precise segmentation, enabling accurate target identification through natural language instructions.

The framework proposes a novel approach for integrating segmentation techniques with vision language models based on multimodal's spatial inference. By leveraging normalized coordinate detection for bounding boxes and translating it into actionable segmentation outputs, we explore the possibility of integrating multimodal's spatial and language representations. Based on the proposed technical approach, the framework demonstrates superior performance on various benchmark datasets as well as accurate object segmentation: COCO 2017 datasets for general object detection and Pascal VOC datasets for semantic segmentation demonstrate the generalization capabilities of the framework.

***K*eywords** Vision Language Understanding, Multimodal Architecture , Spatial Coordinate Detection, Computer Vision

1 Introduction

Recent advancements in multimodal artificial intelligence systems are progressively dissolving the traditional demarcation between computer vision and natural language processing paradigms [1], yielding substantial progress across diverse application domains [2]. Notably, Vision-Language Models (VLMs), through their integration of visual comprehension and natural language processing capabilities [3] [4], have demonstrated remarkable efficacy in various tasks including image caption generation, object recognition, and cross-modal retrieval [5] [6]. Nevertheless, despite these technological strides, fundamental limitations persist in tasks necessitating precise spatial comprehension and segmentation capabilities.

Existing Vision-Language Models (VLMs), while demonstrating remarkable capabilities in general semantic understanding, exhibit limitations in handling spatially explicit tasks [7]. Contemporary approaches predominantly rely on contrastive learning-based embedding methods (e.g., CLIP [2]), which effectively capture overall semantic associations between images and text but demonstrate notable deficiencies in processing specific spatial relationships [8]. For instance, Anomaly GPT [9] employs image decoders to obtain localization results, designs dedicated prompt learners to provide fine-grained semantics for large language models, and utilizes prompt embeddings to fine-tune vision-language

Citation: **Authors. Title. Pages.... DOI:000000/11111.**

models. Similarly, LISA [10] adopts an image decoder architecture trained through natural language descriptions and matched images. However, these approaches exhibit inherent limitations, primarily manifesting in their reliance on descriptive expressions rather than precise localization, fundamentally stemming from the embedding space's lack of explicit spatial information preservation [11]. These limitations become particularly pronounced in real-world applications, such as lesion location identification in medical imaging [12], precise object manipulation in robotics [13], and object position recognition in autonomous vehicles [14]. Such applications demand pixel-level precise spatial recognition rather than approximate position estimation. Furthermore, the absence of effective evaluation mechanisms renders these limitations difficult to assess and improve during model fine-tuning processes.

The precise processing of spatial information encompasses multiple fundamental challenges that warrant systematic investigation [15]. Primarily, the maintenance of consistent spatial reference frameworks across images exhibiting heterogeneous resolutions and scale factors necessitates sophisticated calibration methodologies [4, 8]. Subsequently, there exists a substantial semantic-spatial translation challenge wherein models must bridge the inherent gap between natural language spatial descriptors and precise coordinate-based representations [3, 7]. Furthermore, the development of robust architectural frameworks that simultaneously achieve high spatial precision while maintaining generalizability across diverse operational contexts presents technical complexities [12, 16].

In this study, we present SJTU:Spatial Judgments in Multimodal models - Towards Unified Segmentation through Coordinate Detection, a novel framework that addresses spatial localization challenges in vision-language tasks by representing spatial information through explicit coordinate systems and leveraging Large Language Models (LLMs) [17] to transform natural language descriptions into standardized coordinates. The framework incorporates the Qwen2 Vision-Language model (Qwen2-VL) model [18] for processing user prompts and extracting spatial information, while integrating Segment Anything Model 2 (SAM2) [4] for segmentation tasks. Through the implementation of a standardized coordinate system, SJTU ensures consistent spatial reference across varying image resolutions, achieving pixel-precise object segmentation and offering an end-to-end solution for natural language-guided visual tasks.

The main contributions of this work are summarized as follows:

- We propose a novel methodology that effectively bridges Vision Language Models (VLMs) and segmentation techniques through coordinate-based spatial reasoning.
- We implement consistent spatial referencing through a normalized coordinate system, wherein the integration of Qwen2-VL and SAM2 enables precise object detection and segmentation.
- We validate the efficacy of our proposed method through extensive experimental evaluation on COCO 2017 and Pascal VOC datasets.

The study aims to explore the role of spatial understanding in multimodal artificial intelligence systems and suggests potential approaches to address current limitations in vision-language models. The remainder of this paper is organized as follows: Section 2 examines relevant literature and theoretical foundations, Section 3 describes the proposed methodological framework, Section 4 analyzes experimental results and their implications, and Section 5 discusses our findings and possible directions for future research.

2 Related Work

Recent advances in vision-language models and segmentation techniques have demonstrated strides in multimodal understanding. This section presents a comprehensive review of related work across three fundamental domains: image segmentation, vision-language models and spatial understanding in visual systems.

2.1 Image Segmentation

Image segmentation has made remarkable strides through architectural innovations. Early approaches primarily centered on CNN-based architectures, where FCN [19] pioneered end-to-end learnable segmentation methods, while U-Net [20] achieved precise boundary preservation through skip connections. The DeepLab series [21] [22] advanced the field by leveraging dilated convolutions and efficient multi-scale processing. The emergence of Transformer-based architectures [23] introduced novel perspectives to the segmentation domain, with DETR [24] demonstrating the efficacy of attention mechanisms in visual understanding.

SAM [4] introduced a advancement through its prompt-based universal segmentation framework, leveraging training on billions of masks. This foundation was further enhanced by X-Decoder [25], which integrated multiple interaction modalities, encompassing textual, audio, and scribble-based inputs. Recent investigations [26] [27] have concentrated on instance-level segmentation, incorporating innovative approaches such as mask attention mechanisms and dynamic convolutions to enhance boundary detection precision.

The evolution of segmentation techniques has progressively emphasized human-machine interaction paradigms. Referring segmentation approaches [28] have enabled language-guided object localization, while interactive segmentation methodologies [29] have incorporated diverse user input mechanisms. However, these approaches predominantly rely on rudimentary matching between textual and visual features, lacking explicit spatial reasoning capabilities.

2.2 Vision-Language models

Vision-language models have achieved advancements in recent years. CLIP [2] established robust visual-linguistic alignment through large-scale contrastive learning methodologies, while GPT-4V [30] and LLaVA [16] demonstrated sophisticated visual reasoning capabilities by incorporating visual features into large language models.

Recent developments in vision-language models have primarily focused on establishing more effective connections between visual and linguistic modalities. In this domain, Flamingo [31] pioneered learning in visual contexts through cross-attention architectures, followed by BLIP-2 [7] and mPLUG-OWL [32], which proposed innovative approaches for integrating visual features into language models. Building upon these advances, works such as Otter [33] and MiniGPT-4 [34] further enhanced the models' few-shot capabilities through instruction tuning.

Recent research has demonstrated increasing attention to the intersection of vision-language models and task-specific applications. While models such as VisionLLM [35] and Kosmos-2 [36] have advanced the field by introducing flexible interfaces for vision-centric tasks, DetGPT [37] and GPT4RoI [38] have focused on developing capabilities in spatially-aware detection tasks. However, these approaches predominantly operate in semantic space, exhibiting notable limitations in coordinate-based spatial reasoning, which remains a critical frontier for advancement in vision-language modeling.

2.3 Spatial Understanding in Visual Systems

Spatial understanding in visual systems has undergone an evolution: from traditional approaches that relied on geometric features [39] and rule-based methodologies [40], to the development of graph-based representations [41] and spatial relationship networks for explicit spatial modeling. Recent research has witnessed the convergence of vision-language models with spatial understanding, where LISA innovatively integrates segmentation networks and language models, establishing a novel research direction in this field.

Despite advancements, contemporary vision-language models face several critical limitations. While these models excel in semantic comprehension, they encounter substantial challenges in precise spatial localization. A impediment remains the lack of effective mechanisms for translating natural language spatial descriptions into accurate coordinates. Furthermore, existing approaches often compromise precision in favor of generality when integrating language understanding with segmentation tasks.

To address these limitations, we propose a novel coordinate-based methodology that establishes an effective bridge between natural language instructions and precise segmentation tasks. In contrast to prior approaches that rely on spatial embedding matching or implicit spatial understanding, our framework introduces an explicit coordinate-based mechanism that achieves precise localization while maintaining the semantic comprehension capabilities inherent in large language models.

3 Method

In this work, we present SJTU: Spatial Judgments in Multimodal models - Towards Unified Segmentation through Coordinate Detection, a novel multimodal model framework that achieves precise segmentation based on natural language prompts through the introduction of spatial judgment mechanisms. The key innovation lies in its coordinate-based spatial understanding approach, which effectively bridges the gap between language comprehension and pixel-precise segmentation. In this section, we first present the overall framework architecture, followed by a detailed exposition of its primary technical components and implementation details.

3.1 Overview

Inspired by recent advances in multimodal architectures, SJTU developed a coordinate-based system that integrates visual language understanding with precise segmentation. The system comprises three core components: the SAM2 encoder, SAM2 mask decoder, and Qwen2-VL's vision-language encoder, which work collaboratively to translate natural language commands into accurate segmentation masks.

3.1.1 Vision-Language Integration

Given an input image $x_{\text{img}} \in \mathbb{R}^{H \times W \times 3}$ and text prompt x_{txt}, our dual-encoder architecture processes visual and textual inputs through parallel pathways. The image undergoes dual processing through both SAM2 and Qwen2-VL encoders:

$$f_{\text{img}}^{\text{SAM}} = E_{\text{SAM}}(x_{\text{img}}) \tag{1}$$

$$f_{\text{img}}^{\text{VL}}, f_{\text{txt}} = E_{\text{VL}}(x_{\text{img}}, x_{\text{txt}}) \tag{2}$$

where E_{SAM} represents the SAM2 vision encoder and E_{VL} denotes the Qwen2-VL encoder. Our methodology integrates SAM2's proficiency in precise mask generation with Qwen2-VL's capabilities in vision-language understanding through a coordinate-based mechanism.

The SAM2 pathway (E_{SAM}) employs a hierarchical vision transformer backbone for image processing, extracting fine-grained visual features optimized for segmentation tasks. Concurrently, the Qwen2-VL pathway (E_{VL}) processes both image and text prompts, facilitating cross-modal understanding and spatial reasoning. This dual-pathway architecture enables our system to maintain both precise spatial control and semantic comprehension.

The features extracted through these distinct pathways serve complementary objectives:

- $f_{\text{img}}^{\text{SAM}}$ is preserved for subsequent mask generation
- $f_{\text{img}}^{\text{VL}}$ and f_{txt} are utilized for coordinate prediction via our spatial reasoning module

This architectural strategy implements distinct pathways for segmentation and understanding, wherein SAM2's parameters remain frozen to ensure consistent feature extraction, while the Qwen2-VL component undergoes fine-tuning to optimize coordinate prediction performance.

3.1.2 Coordinate Prediction

Building upon recent advances in spatial understanding, we extend Qwen2-VL's functionality to generate normalized coordinates for precise spatial localization. The coordinate prediction process is formulated as:

$$[x_1, y_1, x_2, y_2] = F_{VL}(f_{img}^{VL}, f_{txt}) \tag{3}$$

where F_{VL} represents the coordinate prediction function. Following common practice in object detection, the coordinates are normalized based on image dimensions:

$$x_{norm} = \frac{x_{raw}}{W}, y_{norm} = \frac{y_{raw}}{H} \tag{4}$$

where W and H represent the width and height of the input image respectively. This normalization maps raw pixel coordinates to $[0, 1]$ range, ensuring scale-invariant representation regardless of input image resolution. For instance, in an image of size 300×200, a bounding box with raw coordinates $[30, 60, 90, 100]$ would be normalized to $[0.1, 0.3, 0.3, 0.5]$.

Our normalized coordinate system was designed to address various challenges encountered during actual experiments. In early tests, the multimodal model showed inconsistent results when dealing with images of different sizes and ratios, with predictions becoming particularly unstable in zero-shot scenarios.

The normalization system we introduced in response to these challenges brought three key advantages. First, the model became capable of producing stable results regardless of input image size. Second, spatial reference points remained consistent across images of varying aspect ratios, improving the accuracy of object location predictions. Finally, integration with downstream segmentation tasks became much smoother, enhancing the overall pipeline efficiency. This system also effectively addressed the hallucination phenomenon sometimes observed in multimodal models, where they would predict coordinates inconsistent with actual image dimensions and ratios.

The coordinate prediction module leverages Qwen2-VL's cross-modal understanding capabilities to transform natural language spatial descriptions into precise coordinate representations, bridging the gap between semantic understanding and spatial localization.

3.1.3 Mask Generation

The final segmentation mask is generated through SAM2's mask decoder. The generation process consists of two steps. First, the normalized coordinates are transformed into prompt embeddings:

$$E_{prompt} = T_{prompt}([x_1, y_1, x_2, y_2]) \in \mathbb{R}^{N \times D} \tag{5}$$

Then, the mask decoder generates the segmentation mask using the image features and prompt embeddings:

$$\hat{M} = D_{mask}(f_{img}^{SAM}, E_{prompt}) \in \mathbb{R}^{H \times W} \tag{6}$$

where D_{mask} represents SAM2's mask decoder, T_{prompt} is the prompt encoder that transforms coordinates into embeddings, E_{prompt} represents the prompt embeddings, and $\hat{M}$ is the predicted binary segmentation mask. The mask decoder utilizes the pre-extracted image features f_{img}^{SAM} and the encoded prompt information to generate the final segmentation mask. To maintain model stability and consistency, we keep the parameters of SAM2's mask decoder frozen during both training and inference stages, ensuring high-quality mask generation results.

The overall architecture of our proposed system is illustrated in Fig. 1, which depicts a dual-pathway design incorporating SAM2 for mask generation and a Multi-Modal LLM for coordinate prediction.

3.1.4 Grid Enhancement Implementation

To enhance the model's spatial comprehension capabilities, we introduce a grid-based visual augmentation methodology that incorporates structured spatial reference patterns into the input images. This enhancement strategy serves as an explicit spatial reference framework for coordinate prediction, facilitating more precise spatial localization.

The implementation methodology involves superimposing a structured grid pattern onto the original image through alpha blending. The grid pattern consists of equidistant horizontal and vertical lines forming a binary mask, where grid lines are represented by black pixels while maintaining transparency elsewhere. The enhanced image is generated through a weighted combination of the original image and the grid pattern, with consideration given to preserve essential visual features.

The grid enhancement is integrated into the preprocessing pipeline, preceding both the SAM2 and Qwen2-VL encoding stages. This implementation strategy ensures minimal computational overhead while providing enhanced spatial reference information to both processing pathways. Additionally, we implement an adaptive grid spacing mechanism that dynamically adjusts according to input image dimensions, ensuring consistent spatial reference density across varying image resolutions.

Through this grid enhancement methodology, we establish a robust framework for spatial reference that improves coordinate prediction accuracy while maintaining computational efficiency. The enhancement procedure introduces negligible computational overhead while providing substantial benefits to spatial understanding capabilities.

3.2 Coordinate-based Spatial Understanding

Unlike previous approaches that rely on attention mechanisms [4] or feature matching [2, 16] for spatial understanding, we introduce a coordinate-based methodology that enables precise spatial control. This method achieves end-to-end mapping from natural language instructions to precise segmentation through explicit coordinate representation and processing.

3.2.1 Coordinate Space Design

Building upon our normalized coordinate system introduced in Section 3.1, we implement additional validation and processing mechanisms to ensure robust spatial understanding:

- **Coordinate validation**: We ensure all predicted coordinates fall within the normalized range [0,1].
- **Resolution adaptation**: We maintain consistent coordinate representations across different image resolutions.
- **Format standardization**: We standardize coordinate outputs through the coordinate processing module to convert them into the required input format for the SAM2 mask decoder.

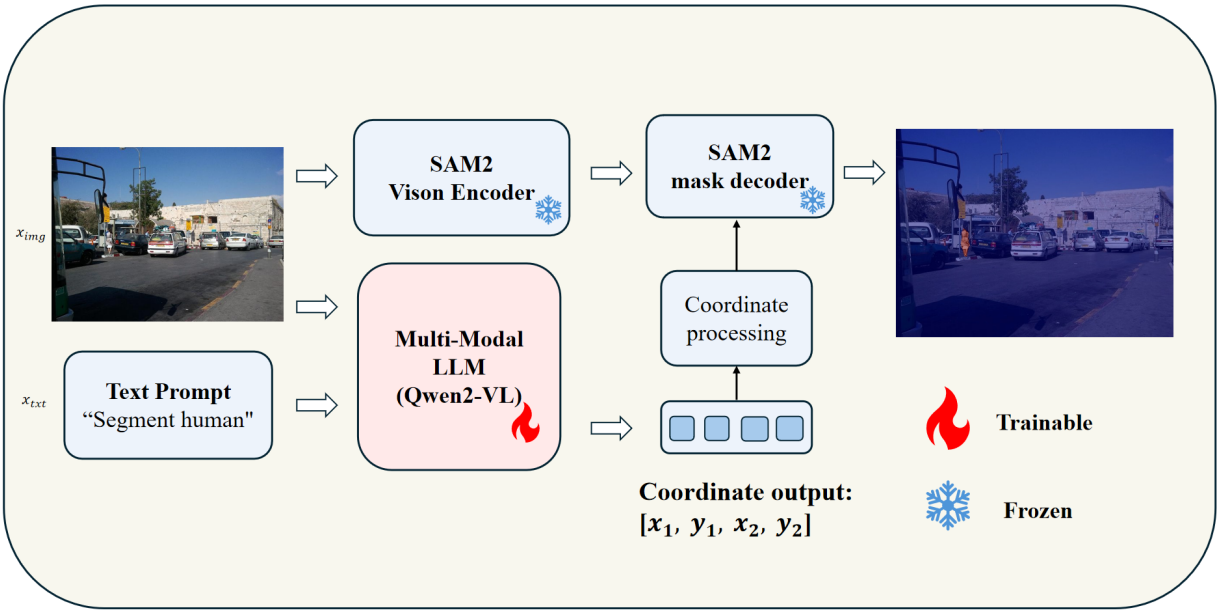

Figure 1: The overall architecture of our coordinate-based image segmentation system. The system consists of two parallel pathways: a frozen SAM2 pathway for precise mask generation and a trainable Multi-Modal LLM pathway for coordinate prediction. The input image (x_{img}) is processed by both pathways, while the text prompt (x_{txt}) is handled by the Multi-Modal LLM. The coordinate output $[x_1, y_1, x_2, y_2]$ from the LLM pathway is processed and fed into the SAM2 mask decoder to generate the final segmentation mask. The snowflake and flame icons indicate frozen and trainable components respectively.

3.2.2 Spatial Reasoning Process

Our spatial reasoning process builds upon recent advances in multimodal understanding [3] while introducing novel coordinate-based control. The specific steps are as follows:

1. Text-guided coordinate prediction using Qwen2-VL:

- Receives natural language instructions and image input
- Generates normalized coordinates through multimodal understanding
- Outputs in format $[x_1, y_1, x_2, y_2]$

2. Coordinate validation and standardization:

- Ensures predicted coordinates within [0,1] range
- Applies coordinate transformation to accommodate different resolutions
- Converts to pixel space coordinates for precise segmentation

This coordinate-based approach not only provides precise spatial control but also establishes a reliable localization foundation for subsequent segmentation tasks. By decoupling language understanding and spatial localization, our system better handles complex vision-language interaction tasks.

3.3 Model Implementation Details

3.3.1 SAM2 Encoder-Decoder Implementation

The SAM2 encoder-decoder architecture in our implementation employs a hierarchical feature extraction and mask generation pipeline. The image encoding process through the Vision Transformer backbone is formalized as:

$$F_{img} = E_{SAM}(x_{img}) \in \mathbb{R}^{H' \times W' \times D} \tag{7}$$

where F_{img} represents the hierarchical feature map with spatial dimensions H' and W', and feature dimension D. The encoder architecture includes:

- A patch embedding layer for initial feature extraction
- Multiple transformer blocks with self-attention mechanisms
- Multi-scale feature aggregation for comprehensive spatial understanding

For coordinate-to-prompt conversion, we implement a two-stage transformation process:

$$P = T_{box}((x_1, y_1, x_2, y_2)) \in \mathbb{R}^4 \tag{8}$$

$$E_{prompt} = T_{prompt}(P) \in \mathbb{R}^{N \times D} \tag{9}$$

where T_{box} standardizes the coordinate format and T_{prompt} converts the standardized coordinates into prompt embeddings suitable for the decoder.

To leverage SAM2's pre-trained capabilities effectively, all encoder and decoder parameters remain frozen, operating in a zero-shot manner. This design choice ensures stable feature extraction and consistent mask generation performance across different application scenarios.The detailed architecture of the SAM2 decoder and its mask generation process are elaborated in Section 3.1.3.

3.3.2 Qwen2-VL Model Configuration

In our implementation, the Qwen2-VL model is primarily responsible for interpreting textual prompts and generating precise spatial coordinates. The attention mechanism with rotary position embeddings (RoPE) can be expressed as:

$$Q_{rot} = Q \cdot e^{im\theta}, K_{rot} = K \cdot e^{im\theta} \tag{10}$$

$$A(Q, K, V) = \text{softmax}(\frac{Q_{rot}K_{rot}^T}{\sqrt{d_k}})V \tag{11}$$

where Q_{rot} and K_{rot} represent the query and key matrices after applying rotary position embeddings, m represents the sequence position, and θ is the rotation angle. The RoPE mechanism enables the model to better capture relative positional relationships in the sequence. To handle spatial information in our vision-language task, we extend the position encoding to incorporate both sequential and spatial dimensions:

$$\theta_{i,j} = \begin{bmatrix} \theta_{seq} \\ \theta_h \\ \theta_w \end{bmatrix} = \begin{bmatrix} f(i, d_{seq}) \\ f(h, d_{spatial}) \\ f(w, d_{spatial}) \end{bmatrix} \tag{12}$$

where $f(\cdot, d)$ is the position encoding function, i represents the sequence position, and (h, w) represent spatial coordinates. This enhanced position encoding scheme helps the model better understand and predict spatial relationships in the input.

To optimize inference efficiency, we implement several optimizations for Qwen2-VL:

- Integration of Flash Attention 2 mechanism, which optimizes memory access patterns and reduces peak memory usage while maintaining the same theoretical complexity
- Implementation of AWQ (Activation-aware Weight Quantization) for model compression, which adaptively determines quantization parameters based on activation patterns:

$$W_q = s \cdot \text{CLIP}(\text{round}(\frac{W}{s}), -q_{max}, q_{max}) \tag{13}$$

where W_q represents the quantized weights, W represents the original weights, s is the scaling factor determined by the activation statistics, and q_{max} is the maximum quantization value determined by the bit width (typically 127 for 8-bit quantization).

3.3.3 Model Interaction Mechanism

The interaction between the two models is facilitated through the coordinate mapping module. The normalized bounding box coordinates output by Qwen2-VL undergo denormalization transformation before being input to SAM2:

$$(x_p^1, y_p^1) = (x_n^1 \times W, y_n^1 \times H) \tag{14}$$

$$(x_p^2, y_p^2) = (x_n^2 \times W, y_n^2 \times H) \tag{15}$$

where (x_p^1, y_p^1) and (x_p^2, y_p^2) represent the top-left and bottom-right corners in pixel-space coordinates respectively, and W and H denote image width and height. The coordinate mapping ensures that the normalized predictions from Qwen2-VL are properly scaled to match SAM2's input requirements.

Through extensive experimentation, we observe that this implementation achieves optimal performance in terms of both computational efficiency and segmentation accuracy. The frozen weights of SAM2 and the efficient coordinate processing mechanism from fine-tuned Qwen2-VL, enable robust performance across diverse application scenarios while maintaining real-time processing capabilities.

4 Experiments and Results

4.1 Datasets

To evaluate the effectiveness of our proposed framework, we conduct experiments on two widely adopted computer vision benchmarks: COCO 2017 [42] and Pascal VOC [43].The computing resources used in the experiment are unified by the RTX3090.

4.1.1 COCO 2017

The COCO (Common Objects in Context) dataset represents a comprehensive benchmark for object detection, instance segmentation, and image captioning tasks. For our experimental evaluation, we utilize a subset of COCO 2017:

- A randomly sampled training set comprising 20,000 images
- A test set consisting of 500 randomly selected images
- Annotations spanning 80 diverse object categories encountered in everyday scenarios
- Rich annotation types including instance segmentation masks, bounding boxes, and natural language descriptions

4.1.2 Pascal VOC

The Pascal VOC 2012 dataset serves as another standard benchmark in computer vision:

- Training set containing 1,464 fully annotated images
- Validation set comprising 1,449 images
- Annotations covering 20 distinct object categories
- Comprehensive annotations including semantic segmentation masks and object bounding boxes

4.2 Evaluation Metrics

To comprehensively evaluate the effectiveness of our proposed coordinate-based spatial understanding framework, we conduct thorough evaluations using multiple complementary metrics. These metrics are selected to assess both the spatial accuracy of our model's predictions and its computational efficiency.

For spatial accuracy evaluation, we primarily utilize three variants of Intersection over Union metrics. The basic **Intersection over Union (IoU)** serves as our fundamental metric:

$$\text{IoU} = \frac{|B_p \cap B_{gt}|}{|B_p \cup B_{gt}|} \tag{16}$$

where B_p and B_{gt} denote the predicted and ground truth bounding boxes respectively, and $|\cdot|$ represents the area. While IoU effectively measures the direct overlap between predictions and ground truth, it has limitations in cases where boxes do not overlap.

To address this limitation, we additionally employ the **Generalized IoU (GIoU)**, which provides a more nuanced evaluation by considering the smallest enclosing box:

$$\text{GIoU} = \text{IoU} - \frac{|C - (B_p \cup B_{gt})|}{|C|} \tag{17}$$

where C represents the smallest rectangular box enclosing both B_p and B_{gt}. GIoU offers a more meaningful measure especially in cases of non-overlapping boxes, making it particularly valuable for evaluating our coordinate prediction accuracy.

For the most comprehensive spatial assessment, we utilize the **Complete IoU (CIoU)**, which further incorporates the distance between central points and aspect ratio consistency:

$$\text{CIoU} = \text{IoU} - \frac{\rho^2(b_p, b_{gt})}{c^2} - \alpha v \tag{18}$$

where $\rho(\cdot)$ represents the Euclidean distance between central points b_p and b_{gt}, c is the diagonal length of the smallest enclosing box, α is a positive trade-off parameter, and v measures the consistency of aspect ratio. CIoU provides the most complete assessment of our model's spatial understanding capabilities.

Beyond spatial accuracy, we also evaluate the computational efficiency through **Average Inference Time**, measuring the average processing time per image across our test sets. This metric is crucial for assessing the practical applicability of our approach in real-world scenarios, where computational resources may be constrained.

In our experiments, these metrics are calculated across all test samples from both COCO and Pascal VOC datasets, providing a comprehensive evaluation of our framework's performance across different scenarios and object categories. The results demonstrate the effectiveness of our coordinate-based approach in achieving both accurate spatial understanding and efficient computation.

4.3 Comparative Experiments

To rigorously evaluate the efficacy of our proposed SJTU framework, we conducted extensive comparative experiments against state-of-the-art vision-language segmentation models. The evaluation encompasses seven competitive baselines: OVSeg, GRES, X-Decoder, SEEM, Grounded-SAM, LISA-7B, and LISA-13B. The comprehensive assessment was performed on both COCO 2017 and VOC-devkit datasets, utilizing four quantitative metrics: Average IoU, Average GIoU, Average CIoU, and Average Inference Time. Furthermore, we investigated the impact of grid-based visual enhancement on model performance.

4.3.1 Experimental Setup

All experiments were conducted on a computing cluster equipped with 8 NVIDIA RTX 3090 GPUs. To ensure fair comparison, we maintained consistent preprocessing protocols across all models, with input images being resized while preserving their aspect ratios. For baseline evaluation, all models were tested using their official implementations and pre-trained weights.

In addition to standard preprocessing, we introduced a grid-enhanced variant where we overlay a 9×9 black grid with 0.3 transparency on the input images before feeding them into the models. This technique was inspired by the observation that explicit spatial reference points could enhance the model's ability to understand and reason about object locations. The grid lines serve as spatial anchors, potentially helping the model better capture relative positions and spatial relationships between objects.

4.3.2 Grid Enhancement Analysis

The addition of the grid overlay proved to be a simple yet effective enhancement to our framework. The key design choices for the grid were:

- **Grid Size**: A 9×9 grid was chosen after experimenting with various configurations, as it provided sufficient spatial granularity without overly cluttering the image.

- **Grid Color**: Black lines were selected for their universal contrast against most image content.
- **Transparency Level**: A transparency value of 0.3 was found to be optimal, making the grid visible enough to serve as a spatial reference while minimizing interference with the original image features.

The grid enhancement was applied consistently across all test images for both datasets, ensuring fair comparison with the baseline results.

4.3.3 Quantitative Results

The comparative results on COCO 2017 and VOC-devkit datasets are presented in Tables 1 and 2. These results showcase both the baseline performance and the enhanced performance with grid overlay.

Method	COCO 2017			VOC-devkit			Time (s)
	IoU	GIoU	CIoU	IoU	GIoU	CIoU	
OVSeg	0.3531	0.3328	0.3215	0.3329	0.3156	0.3047	3
GRES	0.3828	0.3656	0.3523	0.3987	0.3712	0.3695	4
X-Decoder	0.3412	0.3235	0.3128	0.3352	0.3289	0.3056	6
SEEM	0.3389	0.3198	0.3087	0.3218	0.3065	0.2923	8
Grounded-SAM	0.4298	0.4125	0.3998	0.4156	0.3989	0.3857	12
LISA-7B-v1	0.5229	0.5145	0.4692	0.5729	0.5341	0.5132	52
LISA-13B-v1	0.5553	0.4928	0.4803	0.6353	0.5587	0.5303	71
SJTU (ours)	**0.5958**	**0.5661**	**0.5390**	**0.6758**	**0.6661**	**0.6341**	**7**

Table 1: Baseline performance comparison without grid enhancement. All metrics are averaged across the test set.

Method	COCO 2017			VOC-devkit			Time (s)
	IoU	GIoU	CIoU	IoU	GIoU	CIoU	
OVSeg	0.3589	0.3517	0.3472	0.3307	0.3273	0.3187	3
GRES	0.3885	0.3423	0.3305	0.3774	0.3507	0.3451	4
X-Decoder	0.3463	0.3315	0.3278	0.3528	0.3172	0.3167	6
SEEM	0.3440	0.3269	0.3143	0.3293	0.3166	0.2941	8
Grounded-SAM	0.4384	0.4291	0.4317	0.4155	0.4084	0.3949	12
LISA-7B-v1	0.5240	0.5177	0.4704	0.5240	0.5177	0.4704	52
LISA-13B-v1	0.5602	0.5432	0.5192	0.5602	0.5432	0.5192	71
SJTU (ours)	**0.6033**	**0.6874**	**0.5812**	**0.6923**	**0.7642**	**0.6844**	**7**

Table 2: Performance comparison with grid enhancement (9×9 black grid, 0.3 transparency). The grid overlay technique substantially improves performance across all metrics.

As shown in Table 1 and Table 2, our grid-enhanced SJTU framework achieved state-of-the-art performance across both datasets. On COCO 2017, the grid enhancement improved our model's Average IoU from 0.5958 to 0.6033, GIoU from 0.5661 to 0.6874, and CIoU from 0.5390 to 0.5812, surpassing the previous best model LISA-13B by substantial margins. Similar performance advantages were observed on the VOC-devkit dataset, where the grid enhancement improved our model's Average IoU from 0.6758 to 0.6923, GIoU from 0.6661 to 0.7642, and CIoU from 0.6341 to 0.6844. The more substantial improvement on the VOC-devkit dataset suggests that the grid enhancement is particularly effective when dealing with well-defined object boundaries.

4.3.4 Analysis

The experimental results reveal several findings:

- **Grid Enhancement Effect**: The introduction of the 9×9 grid overlay has led to substantial improvements across all metrics compared to our base model. The structured visual cues provided by the grid facilitate more accurate coordinate prediction and spatial relationship modeling, as evidenced by the improvements in GIoU and CIoU scores.
- **Computational Efficiency**: Despite the additional grid overlay preprocessing step, SJTU maintains its computational efficiency with an average inference time of 7 seconds across both datasets, representing

an order of magnitude improvement over existing approaches like LISA-13B (71s) and LISA-7B (52s). The negligible computational overhead of grid addition makes it a practical enhancement for real-world applications.

- **Cross-dataset Consistency**: The performance advantages of grid-enhanced SJTU are maintained across both COCO 2017 and VOC-devkit datasets, with particularly strong results on VOC-devkit. This consistency demonstrates the robustness of our approach and the effectiveness of the grid overlay technique across different data distributions.
- **Grid Impact Analysis**: The structured guidance provided by the 9×9 grid appears to be particularly beneficial for complex spatial understanding tasks. The transparent overlay preserves essential image features while providing additional spatial reference points, leading to more accurate coordinate predictions and improved segmentation quality. The effectiveness of this simple enhancement suggests that explicit spatial cues play a crucial role in visual understanding tasks.

The experimental results validate our hypothesis that explicit coordinate-based spatial understanding, enhanced by structured visual cues, leads to more accurate and efficient segmentation compared to existing approaches. The introduction of the grid overlay technique, while simple in concept, provides substantial improvements in model performance without compromising computational efficiency. The stronger performance on VOC-devkit further suggests that our grid-enhanced approach is particularly effective on datasets with well-defined object boundaries and clear spatial relationships.

4.4 Segmentation Visualization

To demonstrate the effectiveness of our approach, we present qualitative results of our SJTU model's segmentation performance. Figure 2 shows two representative examples with different segmentation scenarios.

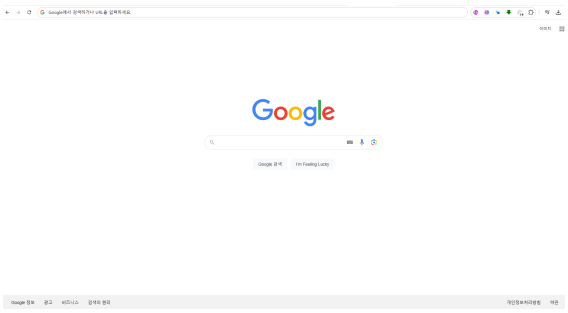

(a) Input Image

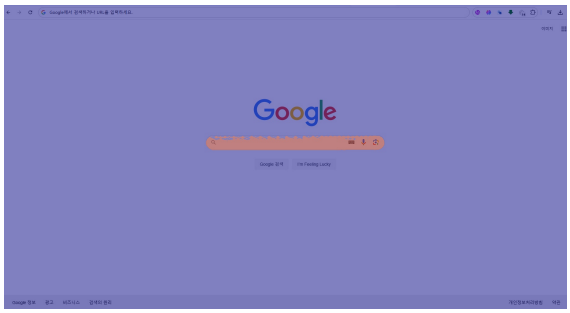

(b) Segment search engine

(c) Input Image

(d) Segment every cars

Figure 2: Visualization of segmentation results by our SJTU model. Different colors represent different object instances. The model demonstrates strong performance in both single-object and multi-object scenarios, accurately capturing object boundaries and maintaining instance separation. (Best viewed in color)

Our model demonstrates robust segmentation capabilities across various scenarios. In the first example (Figures 2a and 2b), the model successfully segments a complex scene with multiple overlapping objects. The segmentation masks

show clear boundary delineation and accurate instance separation, even in areas with challenging visual transitions. The second example (Figures 2c and 2d) further illustrates our model's ability to handle fine-grained details and intricate object structures.

These qualitative results complement our quantitative metrics, showcasing the model's practical effectiveness in real-world scenarios. The visualizations demonstrate that our SJTU model not only achieves strong numerical performance but also produces visually accurate and meaningful segmentations that could be valuable for downstream applications.

5 Discussion

The experimental results demonstrate that our coordinate-based spatial understanding framework offers advantages in vision-language segmentation tasks. In this section, we analyze the broader implications of our findings, discuss the limitations of our approach, and explore potential future research directions.

5.1 Analysis of Framework Performance

Our framework's superior performance can be attributed to several key factors:

- **Coordinate-based Spatial Understanding**: The explicit coordinate representation bridges the gap between natural language understanding and precise segmentation, providing a more direct and interpretable approach compared to traditional attention-based methods. This approach enables more accurate spatial localization while maintaining semantic understanding capabilities.
- **Grid Enhancement Effects**: The introduction of the grid overlay technique demonstrates that providing explicit spatial reference points improves model performance. The consistent improvement across different datasets suggests that structured visual cues play a crucial role in enhancing spatial understanding capabilities. This finding has broader implications for the design of vision-language architectures.
- **Computational Efficiency**: Our framework achieves state-of-the-art performance while maintaining lower inference times compared to existing approaches. This efficiency stems from our architectural design choices, particularly the separation of coordinate prediction and mask generation pathways.

5.2 Limitations and Challenges

Despite the strong performance of our framework, several limitations warrant discussion:

- **Resolution Dependency**: While our normalized coordinate system addresses many scale-invariance issues, the effectiveness of the grid enhancement technique may vary with image resolution. Future work could explore adaptive grid densities based on image characteristics.
- **Complex Spatial Relationships**: The current framework primarily focuses on bounding box-based localization. Handling more complex spatial relationships (e.g., "between," "behind," "partially occluded") remains challenging and requires further investigation.
- **Language Ambiguity**: Natural language descriptions of spatial relationships can be inherently ambiguous. Our current approach may struggle with imprecise or contextually dependent spatial references, suggesting the need for more sophisticated language understanding mechanisms.

5.3 Future Research Directions

Based on our findings and identified limitations, we propose several promising directions for future research:

- **Dynamic Grid Enhancement**: Investigating adaptive grid patterns that adjust based on image content and task requirements could further improve spatial understanding capabilities. This might include varying grid densities or incorporating learned grid patterns.
- **Extended Coordinate Representations**: Expanding the coordinate system to handle more complex spatial relationships and three-dimensional understanding could broaden the framework's applicability to more challenging scenarios.
- **Multi-modal Integration**: Exploring the integration of additional modalities (e.g., depth information, temporal sequences) could enhance the framework's ability to understand and reason about spatial relationships in more complex environments.

- **Real-world Applications**: Investigating the framework's performance in specific application domains such as medical imaging, autonomous navigation, and robotic manipulation could lead to specialized architectural improvements and domain-specific optimizations.

5.4 Broader Implications

Our research has several important implications for the field of artificial intelligence:

- **Architectural Design**: The success of our coordinate-based approach suggests that explicit spatial representations might be beneficial for other vision-language tasks beyond segmentation. This could influence the design of future multimodal architectures.
- **Human-AI Interaction**: The improved spatial understanding capabilities demonstrated by our framework could enhance human-AI interaction in applications requiring precise spatial communication, such as robotic control or augmented reality systems.
- **Computational Efficiency**: Our framework's ability to achieve state-of-the-art performance with reduced computational requirements suggests that architectural optimization might be more effective than simply scaling model size.

6 Conclusion

In this paper, we introduce SJTU, a novel framework that bridges vision-language understanding and precise segmentation through coordinate-based spatial reasoning. Our approach demonstrates that explicit coordinate representation, enhanced by grid-based visual augmentation, can improve the accuracy and efficiency of multimodal segmentation tasks. The experimental results across COCO 2017 and Pascal VOC datasets validate the effectiveness of our methodology, achieving state-of-the-art performance while maintaining substantially lower computational requirements compared to existing approaches.

The success of our coordinate-based approach opens new avenues for research in vision-language interaction, suggesting that explicit spatial representations and structured visual cues play crucial roles in enhancing multimodal understanding. As the field continues to evolve, we anticipate that the principles and methodologies introduced in this paper will contribute to the development of more sophisticated and efficient multimodal artificial intelligence systems, particularly in applications requiring precise spatial understanding such as medical imaging, autonomous systems, and human-robot interaction.

References

[1] Danny Driess, Fei Xia, Mehdi SM Sajjadi, Corey Lynch, Aakanksha Chowdhery, Brian Ichter, Ayzaan Wahid, Jonathan Tompson, Quan Vuong, Tianhe Yu, et al. Palm-e: An embodied multimodal language model. *arXiv preprint arXiv:2303.03378*, 2023.

[2] Alec Radford, Jong Wook Kim, Chris Hallacy, Aditya Ramesh, Gabriel Goh, Sandhini Agarwal, Girish Sastry, Amanda Askell, Pamela Mishkin, Jack Clark, et al. Learning transferable visual models from natural language supervision. In *International conference on machine learning*, pages 8748–8763. PMLR, 2021.

[3] Xi Chen, Xiao Wang, Soravit Changpinyo, AJ Piergiovanni, Piotr Padlewski, Daniel Salz, Sebastian Goodman, Adam Grycner, Basil Mustafa, Lucas Beyer, et al. Pali: A jointly-scaled multilingual language-image model. *arXiv preprint arXiv:2209.06794*, 2022.

[4] Alexander Kirillov, Eric Mintun, Nikhila Ravi, Hanzi Mao, Chloe Rolland, Laura Gustafson, Tete Xiao, Spencer Whitehead, Alexander C Berg, Wan-Yen Lo, et al. Segment anything. In *Proceedings of the IEEE/CVF International Conference on Computer Vision*, pages 4015–4026, 2023.

[5] Shaohan Huang, Li Dong, Wenhui Wang, Yaru Hao, Saksham Singhal, Shuming Ma, Tengchao Lv, Lei Cui, Owais Khan Mohammed, Barun Patra, et al. Language is not all you need: Aligning perception with language models. *Advances in Neural Information Processing Systems*, 36:72096–72109, 2023.

[6] Junnan Li, Dongxu Li, Caiming Xiong, and Steven Hoi. Blip: Bootstrapping language-image pre-training for unified vision-language understanding and generation. In *International conference on machine learning*, pages 12888–12900. PMLR, 2022.

[7] Junnan Li, Dongxu Li, Silvio Savarese, and Steven Hoi. Blip-2: Bootstrapping language-image pre-training with frozen image encoders and large language models. In *International conference on machine learning*, pages 19730–19742. PMLR, 2023.

[8] Kaiyang Zhou, Jingkang Yang, Chen Change Loy, and Ziwei Liu. Learning to prompt for vision-language models. *International Journal of Computer Vision*, 130(9):2337–2348, 2022.

[9] Zhaopeng Gu, Bingke Zhu, Guibo Zhu, Yingying Chen, Ming Tang, and Jinqiao Wang. Anomalygpt: Detecting industrial anomalies using large vision-language models. In *Proceedings of the AAAI Conference on Artificial Intelligence*, volume 38, pages 1932–1940, 2024.

[10] Xin Lai, Zhuotao Tian, Yukang Chen, Yanwei Li, Yuhui Yuan, Shu Liu, and Jiaya Jia. Lisa: Reasoning segmentation via large language model. In *Proceedings of the IEEE/CVF Conference on Computer Vision and Pattern Recognition*, pages 9579–9589, 2024.

[11] Jiaqi Wang, Zihao Wu, Yiwei Li, Hanqi Jiang, Peng Shu, Enze Shi, Huawen Hu, Chong Ma, Yiheng Liu, Xuhui Wang, et al. Large language models for robotics: Opportunities, challenges, and perspectives. *arXiv preprint arXiv:2401.04334*, 2024.

[12] Prashant Shrestha, Sanskar Amgain, Bidur Khanal, Cristian A Linte, and Binod Bhattarai. Medical vision language pretraining: A survey. *arXiv preprint arXiv:2312.06224*, 2023.

[13] Fanlong Zeng, Wensheng Gan, Yongheng Wang, Ning Liu, and Philip S Yu. Large language models for robotics: A survey. *arXiv preprint arXiv:2311.07226*, 2023.

[14] Zhenjie Yang, Xiaosong Jia, Hongyang Li, and Junchi Yan. Llm4drive: A survey of large language models for autonomous driving. In *NeurIPS 2024 Workshop on Open-World Agents*, 2023.

[15] Chenfei Wu, Shengming Yin, Weizhen Qi, Xiaodong Wang, Zecheng Tang, and Nan Duan. Visual chatgpt: Talking, drawing and editing with visual foundation models. *arXiv preprint arXiv:2303.04671*, 2023.

[16] Haotian Liu, Chunyuan Li, Qingyang Wu, and Yong Jae Lee. Visual instruction tuning. *Advances in neural information processing systems*, 36, 2024.

[17] Tom B Brown. Language models are few-shot learners. *arXiv preprint arXiv:2005.14165*, 2020.

[18] Jinze Bai, Shuai Bai, Shusheng Yang, Shijie Wang, Sinan Tan, Peng Wang, Junyang Lin, Chang Zhou, and Jingren Zhou. Qwen-vl: A versatile vision-language model for understanding, localization, text reading, and beyond. *arXiv preprint arXiv:2308.12966*, 1(2):3, 2023.

[19] Jonathan Long, Evan Shelhamer, and Trevor Darrell. Fully convolutional networks for semantic segmentation. In *Proceedings of the IEEE conference on computer vision and pattern recognition*, pages 3431–3440, 2015.

[20] Olaf Ronneberger, Philipp Fischer, and Thomas Brox. U-net: Convolutional networks for biomedical image segmentation. In *Medical image computing and computer-assisted intervention–MICCAI 2015: 18th international conference, Munich, Germany, October 5-9, 2015, proceedings, part III 18*, pages 234–241. Springer, 2015.

[21] Liang-Chieh Chen. Semantic image segmentation with deep convolutional nets and fully connected crfs. *arXiv preprint arXiv:1412.7062*, 2014.

[22] Liang-Chieh Chen. Rethinking atrous convolution for semantic image segmentation. *arXiv preprint arXiv:1706.05587*, 2017.

[23] Enze Xie, Wenhai Wang, Zhiding Yu, Anima Anandkumar, Jose M Alvarez, and Ping Luo. Segformer: Simple and efficient design for semantic segmentation with transformers. *Advances in neural information processing systems*, 34:12077–12090, 2021.

[24] Nicolas Carion, Francisco Massa, Gabriel Synnaeve, Nicolas Usunier, Alexander Kirillov, and Sergey Zagoruyko. End-to-end object detection with transformers. In *European conference on computer vision*, pages 213–229. Springer, 2020.

[25] Xueyan Zou, Zi-Yi Dou, Jianwei Yang, Zhe Gan, Linjie Li, Chunyuan Li, Xiyang Dai, Harkirat Behl, Jianfeng Wang, Lu Yuan, et al. Generalized decoding for pixel, image, and language. In *Proceedings of the IEEE/CVF Conference on Computer Vision and Pattern Recognition*, pages 15116–15127, 2023.

[26] Bowen Cheng, Ishan Misra, Alexander G Schwing, Alexander Kirillov, and Rohit Girdhar. Masked-attention mask transformer for universal image segmentation. In *Proceedings of the IEEE/CVF conference on computer vision and pattern recognition*, pages 1290–1299, 2022.

[27] Jitesh Jain, Jiachen Li, Mang Tik Chiu, Ali Hassani, Nikita Orlov, and Humphrey Shi. Oneformer: One transformer to rule universal image segmentation. In *Proceedings of the IEEE/CVF Conference on Computer Vision and Pattern Recognition*, pages 2989–2998, 2023.

[28] Jiannan Wu, Yi Jiang, Peize Sun, Zehuan Yuan, and Ping Luo. Language as queries for referring video object segmentation. In *Proceedings of the IEEE/CVF Conference on Computer Vision and Pattern Recognition*, pages 4974–4984, 2022.

[29] Qin Liu, Zhenlin Xu, Gedas Bertasius, and Marc Niethammer. Simpleclick: Interactive image segmentation with simple vision transformers. In *Proceedings of the IEEE/CVF International Conference on Computer Vision*, pages 22290–22300, 2023.

[30] Zhengyuan Yang, Linjie Li, Kevin Lin, Jianfeng Wang, Chung-Ching Lin, Zicheng Liu, and Lijuan Wang. The dawn of lmms: Preliminary explorations with gpt-4v (ision). *arXiv preprint arXiv:2309.17421*, 9(1):1, 2023.

[31] Jean-Baptiste Alayrac, Jeff Donahue, Pauline Luc, Antoine Miech, Iain Barr, Yana Hasson, Karel Lenc, Arthur Mensch, Katherine Millican, Malcolm Reynolds, et al. Flamingo: a visual language model for few-shot learning. *Advances in neural information processing systems*, 35:23716–23736, 2022.

[32] Qinghao Ye, Haiyang Xu, Guohai Xu, Jiabo Ye, Ming Yan, Yiyang Zhou, Junyang Wang, Anwen Hu, Pengcheng Shi, Yaya Shi, et al. mplug-owl: Modularization empowers large language models with multimodality. *arXiv preprint arXiv:2304.14178*, 2023.

[33] Bo Li, Yuanhan Zhang, Liangyu Chen, Jinghao Wang, Jingkang Yang, and Ziwei Liu. Otter: A multi-modal model with in-context instruction tuning, 2023.

[34] Deyao Zhu, Jun Chen, Xiaoqian Shen, Xiang Li, and Mohamed Elhoseiny. Minigpt-4: Enhancing vision-language understanding with advanced large language models. *arXiv preprint arXiv:2304.10592*, 2023.

[35] Wenhai Wang, Zhe Chen, Xiaokang Chen, Jiannan Wu, Xizhou Zhu, Gang Zeng, Ping Luo, Tong Lu, Jie Zhou, Yu Qiao, et al. Visionllm: Large language model is also an open-ended decoder for vision-centric tasks. *Advances in Neural Information Processing Systems*, 36, 2024.

[36] Zhiliang Peng, Wenhui Wang, Li Dong, Yaru Hao, Shaohan Huang, Shuming Ma, and Furu Wei. Kosmos-2: Grounding multimodal large language models to the world. *arXiv preprint arXiv:2306.14824*, 2023.

[37] Renjie Pi, Jiahui Gao, Shizhe Diao, Rui Pan, Hanze Dong, Jipeng Zhang, Lewei Yao, Jianhua Han, Hang Xu, Lingpeng Kong, et al. Detgpt: Detect what you need via reasoning. *arXiv preprint arXiv:2305.14167*, 2023.

[38] Shilong Zhang, Peize Sun, Shoufa Chen, Min Xiao, Wenqi Shao, Wenwei Zhang, Yu Liu, Kai Chen, and Ping Luo. Gpt4roi: Instruction tuning large language model on region-of-interest. *arXiv preprint arXiv:2307.03601*, 2023.

[39] Frédéric Jurie and Cordelia Schmid. Scale-invariant shape features for recognition of object categories. In *Proceedings of the 2004 IEEE Computer Society Conference on Computer Vision and Pattern Recognition, 2004. CVPR 2004.*, volume 2, pages II–II. IEEE, 2004.

[40] Ahmed M. Darwish and Anil K. Jain. A rule based approach for visual pattern inspection. *IEEE Transactions on Pattern Analysis and Machine Intelligence*, 10(1):56–68, 1988.

[41] Danfei Xu, Yuke Zhu, Christopher B Choy, and Li Fei-Fei. Scene graph generation by iterative message passing. In *Proceedings of the IEEE conference on computer vision and pattern recognition*, pages 5410–5419, 2017.

[42] Tsung-Yi Lin, Michael Maire, Serge Belongie, James Hays, Pietro Perona, Deva Ramanan, Piotr Dollár, and C Lawrence Zitnick. Microsoft coco: Common objects in context. In *European conference on computer vision*, pages 740–755. Springer, 2014.

[43] Mark Everingham, Luc Van Gool, Christopher KI Williams, John Winn, and Andrew Zisserman. The pascal visual object classes (voc) challenge. *International journal of computer vision*, 88(2):303–338, 2010.